RJC

RASĀYAN *J. Chem.*
Vol. 18 | No. 1 |531-537| January - March | 2025
ISSN: 0974-1496 | e-ISSN: 0976-0083 | CODEN: RJCABP
http://www.rasayanjournal.com
http://www.rasayanjournal.co.in

MOLECULAR DOCKING AND DYNAMICS ANALYSIS OF α, β, and γ-MANGOSTINS ON TNF-α FOR DISCOVERY OF OSTEOARTHRITIS AGENT

A. Tang[1,✉], D.S.F. Ramadhan[2], R. Dewi[2], R. Muntu[3] and Nurisyah[2]
[1]Department of Physiotherapy, Poltekkes Kemenkes Makassar, Makassar, Indonesia
[2]Department of Pharmacy, Poltekkes Kemenkes Makassar, Makassar, Indonesia
[3]Department of Environmental Health, Poltekkes Kemenkes Makassar, Makassar, Indonesia
✉Corresponding author: acotang@poltekkes-mks.ac.id

ABSTRACT

Osteoarthritis (OA) is a progressive joint disease characterized by cartilage degradation and inflammation, with TNF-α playing a crucial role in promoting inflammatory responses associated with the condition. This research examines the molecular interactions between TNF-α and α, β, and γ-mangostins to evaluate their potential as supportive agents in cryotherapy for managing OA. Molecular docking simulations were performed to evaluate the binding affinity and interaction profiles of these mangostin derivatives with the TNF-α receptor. Results indicate that γ-MG exhibited the highest binding affinity and most favorable interaction with key amino acids in the TNF-α receptor's active site, closely mimicking the interactions observed with the native ligand. In contrast, α-MG and β-MG showed lower binding affinities due to less optimal hydrogen bonding and hydrophobic interactions. The findings suggest that γ-MG, in particular, holds promise as a potent TNF-α inhibitor, potentially enhancing the anti-inflammatory effects of cryotherapy in OA. This study provides a molecular basis for the development of mangosteen-based auxiliary agents in cryotherapy, offering a novel therapeutic approach for OA management.

Keywords: Osteoarthritis, Inflammation, Natural Product, Molecular Docking, Molecular Dynamics, Mangostin.
RASĀYAN*J. Chem.*, Vol. 18, No.1, 2025

INTRODUCTION

Continuous deterioration and devastation of cartilage is the hallmark of osteoarthritis (OA), a common kind of arthritis. This ailment has become a primary contributor to adult disability, affecting millions of people worldwide. It has been determined that one of the contributing factors of OA is disruption in chondrocyte metabolism. To create efficient treatment plans, more study is necessary as the precise mechanisms driving OA are yet unknown.[1] One important inflammatory cytokine that is essential to the inflammatory process is TNF-α.[2] In addition to other inflammatory markers, it promotes the synthesis of several matrix metalloproteinases, including MMP-13, ADAMTS-5, and ADAMTS-7. TNF-α increases its proinflammatory effects by activating the NF-κB signaling pathway.

According to a recent study, TNF-α has a role in the cartilage degradation linked to osteoarthritis. The particular mechanisms underlying the relationship between CST and TNF-α signaling in inflammatory reactions are still unclear.[3] The aim of this work was to evaluate the possibility of CST as a therapeutic method for reducing cartilage deterioration in OA by investigating its interaction with the TNF-α/TNFR signaling system.[4] Many traditional medicines have proven effective in modern treatments, and an increasing amount of research is confirming the therapeutic benefits of natural materials. Furthermore, natural materials are often more affordable and widely available, especially in areas with abundant natural resources, making them an attractive alternative for drug development in developing countries.[5]

In the present study, mangostin isolate investigated the inhibitory effects, specifically α, β, and γ-mangostins (α-MG, β-MG, and γ-MG), isolated from the pericarp of mangosteen, both in vitro and in vivo.[6] In vitro analysis demonstrated that α-MG, β-MG, and γ-MG effectively suppressed the secretion of pro-inflammatory cytokines TNF-α and IL-6 from U937 cells.[2] Complementary *in vivo* studies revealed that mangosteen extract significantly reduced LPS-induced TNF-α levels in mouse plasma. These findings suggest the potential of mangosteen-derived compounds as therapeutic agents for inflammatory conditions and arthritis.

http://doi.org/10.31788/RJC.2025.1819104

In this study, we investigated the molecular mechanisms of three types of mangostin, α-MG, β-MG, and γ-MG, by *in silico* analysis.[7] This study aims to understand the molecular interactions and anti-inflammatory effects of these compounds and evaluate their potential as therapeutic agents in the treatment of inflammatory conditions and arthritis.

EXPERIMENITAL

Hardware and Software

The system is comprised of an Intel (R) Core i5-12500 CPU @ 4.30GHz (8CPUs) processor, a PC with a 2TB hard drive, 120GB solid-state drive, and 16GB RAM. The computer runs Linux Ubuntu 16.04 and Windows 7 and is equipped with Gaussian 09, Gauss View 5.0.8, AutoDock 4.2 equipped with MGLTools 1.5.6, BIOVIA Discovery Studio Visualizer 2016, GROMACS 2016.3, ACPYPE, ForceGen 0.4, VMD 1.9.2, and MMPBSA.py.

Ligand Preparation

The three-dimensional structure of metabolite which serves as the ligand was obtained from the Knapsack database https://www.knapsackfamily.com/knapsack_core/.[8]

Target Receptor Preparation

The three-dimensional crystal structure of TNF-alpha complexed with a small molecule inhibitor (PDB ID: 2AZ5), used as the target protein, was retrieved from the RCSB PDB website at https://www.rscb.org/pdb. The resolution of the receptor was 2.1 Å.[9]

Molecular Docking Analysis

The active site of the receptor was identified using Discovery Studio Visualizer by mapping the catalytic residues. These catalytic residues were then input into Autodock4 software for molecular docking simulations. During receptor preparation, polar hydrogens and Kollman charges were added after removing water molecules and the native ligand.[10,11] All procedures were carried out using AutoDock 4.2.

Dynamics Simulation of Ligand

Various computational methods were employed to ensure accuracy in the molecular dynamics simulation of protein-ligand complexes using Gromacs 2016.3 software.[12] The initial topology and ligand parameters were generated, and both the protein and ligand were treated with the AMBER99SB-ILDN force field.[13,14] To enhance precision, electrostatic interactions were calculated using the Ewald Particle Mesh method. Na+ and Cl- ions were introduced for neutralization, and solvation was performed using the TIP3P water model.[15] The simulation began with a 10,000-step energy minimization, split into 5,000 steps using the steepest descent method and 5,000 steps with the conjugate gradient approach.

The system was then gradually heated over 100 ps to 310 K[16], with temperature controlled by Langevin dynamics.[17] The main production phase was conducted at a constant pressure of one atmosphere and a temperature of 310 K. Hydrogen bonds was constrained using the SHAKE algorithm, with a time step of 2 fs.[18] Over the course of the 200 ns (200,000 ps) simulation, trajectory coordinates were recorded at 20ps intervals.[10,19]

Several analyses were performed, including solvent-accessible surface area (SASA), radial distribution function (RDF), root mean square deviation (RMSD), radius of gyration (Rg), and changes in secondary structure.[20,21] These analyses provided valuable insights into the stability and dynamic behavior of the protein-ligand complex throughout the simulation.

Computational MM-PBSA Binding Free Energy

For the computation of Molecular Mechanics-Poisson-Boltzmann Surface Area (MM/PBSA), the Gromacs 2016.3 software's g_mmpbsa module was utilized[12]. At intervals of ten seconds, an average of one hundred snapshots covering the MD trajectory from 0 to 100 ns were taken.[22] Using a 0.5 Å grid size, the Poisson-Boltzmann equation was utilized to determine the polar desolvation energy.[23] The nonpolar energy contribution was calculated by computing the solvent-accessible surface area with a solvent radius of 1.4 Å. The solvent's dielectric constant was set to 80, which represents water. Next, a thorough evaluation of the protein-ligand-free energy was carried out.

RESULTS AND DISCUSSION

Binding Energy of Ligand-Receptor

Molecular docking analysis was conducted to assess the binding affinity of various compounds to the target receptor, with the goal of evaluating the inhibitory potential of each ligand. Key parameters such as binding energy and inhibition constant (KI) were utilized to evaluate the interactions (Table-1). The native ligand, as the main comparator, showed a binding energy of -9.35 Kcal/mol and a KI of 140.07 nM. A more negative binding energy value indicates a high binding affinity, signifying a stable interaction between the ligand and the target receptor. The low KI, in the nanomolar range, strengthens the indication that the native ligand has a highly effective inhibitory capacity. αM and βM have binding energies of -6.42 Kcal/mol and -6.7 Kcal/mol, respectively. The higher binding energy (less negative) than the native ligand indicates that αM and βM have lower binding affinity. γM showed more promising results compared to the other analogs, with a binding energy of -7.16 Kcal/mol and KI of 5.68 μM. Among the three mangostin analogs tested, γM had the lowest binding energy and the smallest KI, indicating that γM has better binding affinity than alpha and beta-mangostin.

Table-1: The Energy of Ligand Binding with HELA Cell Receptors

Ligand	Binding Energy (Kcal/mol)	KI
αM	-6.42	19.68 uM
βM	-6.7	12.29 uM
γM	-7.16	5.68 uM

Amino Acid Interaction

Fig.-1 illustrates the interactions between native ligands and mangostin analogs with the TNF-alpha receptor, involving various amino acid residues in the active site of the receptor. Differences in the types of interacting amino acids can affect the stability and binding affinity of each ligand to the receptor. Native ligands interact with amino acid residues through conventional hydrogen bonding and hydrophobic interactions. Residue GLY121 is involved in hydrogen bonding, while interactions with hydrophobic residues are formed with 4 residues namely LEU55, VAL123, LEU57, and TYR119. Alpha-mangostin hydrogen bonded with 4 amino acid residues different from the native ligand and 6 hydrophobic interactions were formed.

Alpha-mangostin tends to interact more with polar residues than native ones. Beta-mangostin and gamma-mangostin showed similar interaction patterns to alpha-mangostin, which were stronger with hydrophobic residues as the native ligand. However, gamma-mangostin interacts less with polar residues than the other analogs. Thus, it appears that gamma-mangostin is the analog that is closest to the interaction pattern of the native ligand.

Molecular Dynamics Simulation

RMSD and RMSF Evaluation of Mangostin Ligands-TNF-α Complex

The dynamic stability of native, C10, and C11 was evaluated using molecular dynamics (MD) simulations for 100 ns. The resulting Root Mean Square Deviation (RMSD) graph is shown in Fig.-2. The RMSD trajectory of the receptor complex with αM, βM, and γM on the TNF-α receptor (shown by the graph in Fig.-2). The RMSD data showed that during the simulation, the three ligands had varying fluctuations. In their configuration in the receptor, the βM ligand showed better stability than the other two ligands as indicated by the low RMSD value of 0.1-0.3 Å. While βM and γM ligands show fluctuations above it.Furthermore, the Root Mean Square Fluctuation (RMSF) graph (Fig.-3) shows the protein residues interacting with αM, βM, and γM ligands during 100 ns of molecular dynamics simulation. The RMSF is used to calculate the average deviation of each protein residue location from its average position during the simulation. Greater flexibility or dynamic properties of the residues are indicated by higher RMSF values, while greater stability is indicated by lower values. Along the protein residues with ligands αM (purple line), βM (yellow line), and γM (red line) in the graph, a similar pattern of variation is observed. However, sequences 131-151, which is the region where the ligand binds, show a larger variation of fluctuation in the residue position than the others. It can be seen that βM in that area shows the lowest fluctuation compared to other ligands, which indicates its strong binding stability.

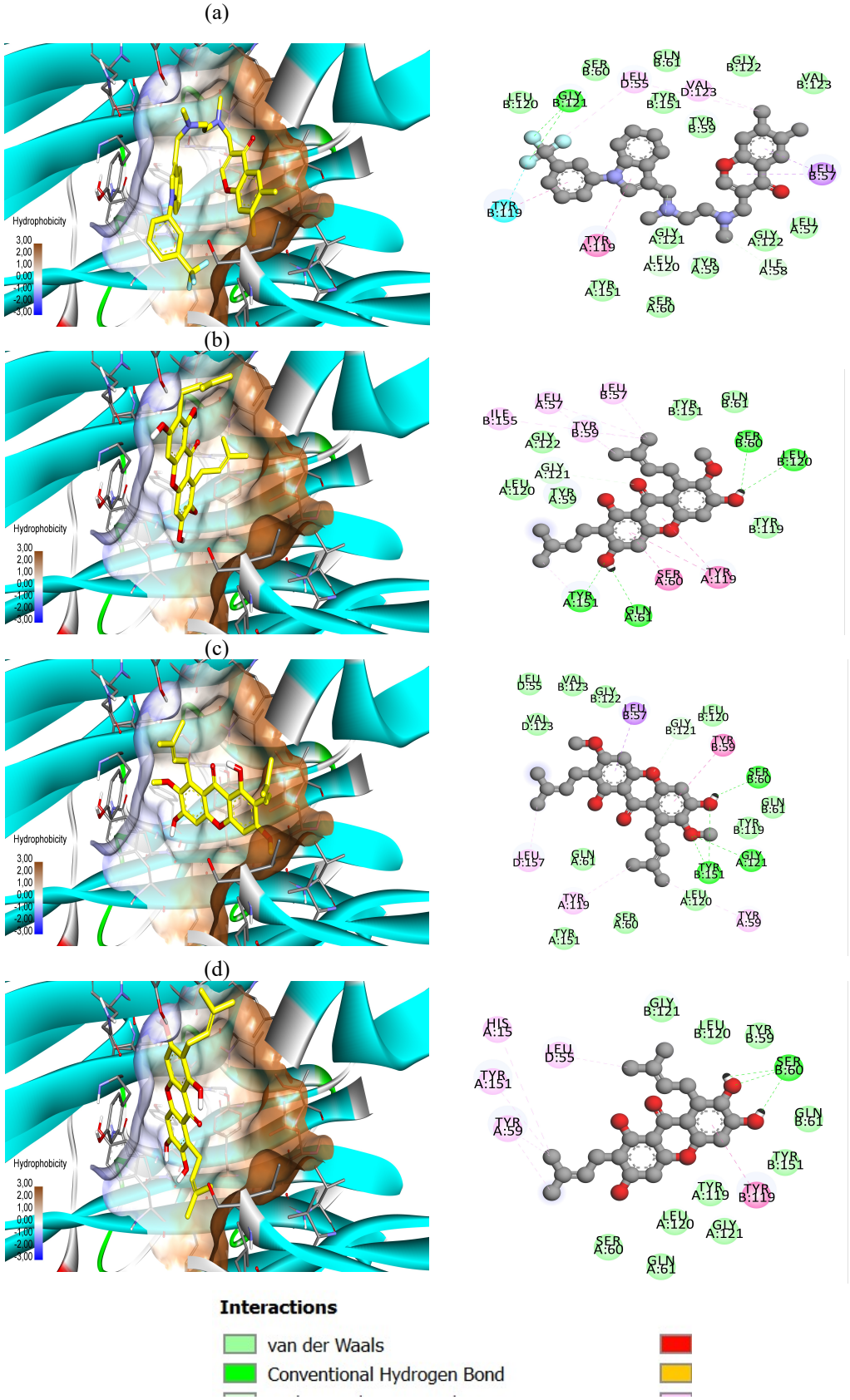

Fig.-1: Amino Acid Interaction of Native Ligand (a), Alpha-Mangostin (b), Beta-Mangostin (c), Gamma-Mangostin (d) in TNF-Alpha Receptor

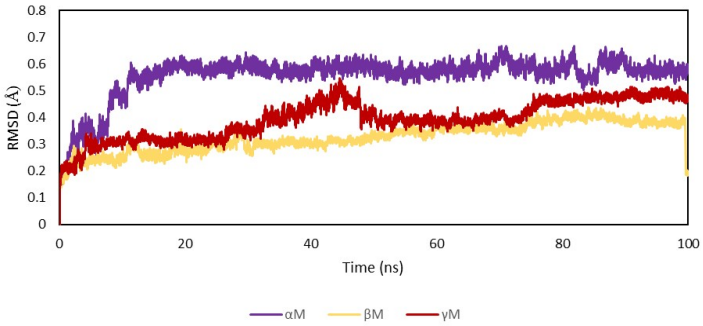

Fig.-2: RMSD Evaluation of αM, βM, and γM in Complex with TNF-α

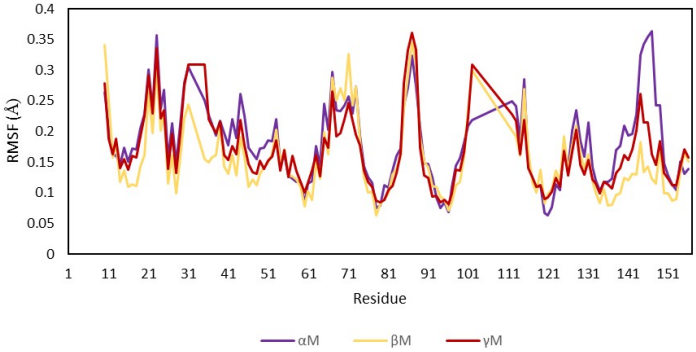

Fig.-3: RMSF Evaluation of αM, βM, and γM in Complex with TNF-α

SASA Evaluation of Mangostin Ligands-TNF-α Complex

Figure-4 shows a graph demonstrating the change in solvent-accessible surface area (SASA) over 10,000 picoseconds (ps) on TNF-α at α, β, and γM. The surface area of a protein exposed to solvent is measured by SASA, and variations in SASA can reveal details about protein stability and structural dynamics. As observed in the graph, there are fluctuations in solvent-exposed surface area during the simulation for αM (purple line), βM (yellow line), and γM (red line). In terms of average value, the SASA for γM is slightly larger than that of αM and βM, which is 248 nm^2 for αM, 251 nm^2 for βM, and 247 nm^2 for γM. This result implies that the three ligands, especially αM and γM are superior to βM in SASA evaluation. However, throughout the simulation, the SASA for the three ligands actually showed very similar fluctuations. This is a benchmark that indicates the three complexes are conformationally stable based on the SASA values and may reduce the possibility of disruptive interactions such as denaturation or aggregation.

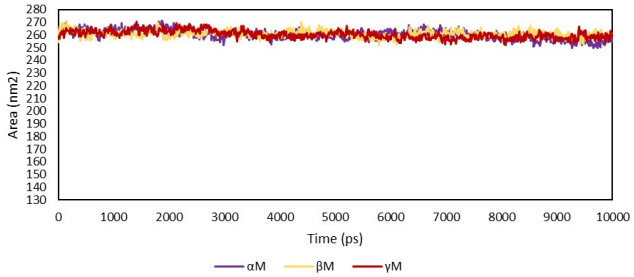

Fig.-4: SASA Evaluation of αM, βM, and γM in Complex with TNF-α

Mangostine Ligands Binding Free Energy

In this TNF-α receptor, we compared the binding free energy components for the three ligands αM, βM, and γM (Table-2). Molecular Mechanics Poisson-Boltzmann Surface Area (MM-PBSA) calculations were performed to measure the stability and binding affinity between the three ligands.[24] The overall picture of ligand binding affinity is given by the total binding free energy, which is the sum of all energy contributions, including Van der Waals energy, electrostatic energy, polar solvation energy, and solvent accessible surface area energy (SAS). The binding free energy of αM is -148.997 kJ/mol, that of βM

ligand is -148.560 KJ/mol, and that of γM is -132.167 KJ/mol. This important difference indicates that αM and βM ligands exhibit much stronger binding energies than γM toward the TNF-α receptor.

Table-2: Results of the Energy Summation of the MM-PBSA Calculations for the Human Receptor TNF-α with αM, βM, and γM Ligands

Molecule Complex	Van der Waals	Electrostatic	Polar Solvation	SASA	Bond Prediction
	Energy (kJ/mol)	Energy (kJ/mol)	Energy (kJ/mol)	Energy (kJ/mol)	Energy (kJ/mol)
αM	-186.124 +/- 11.993	-15.136 +/- 4.904	69.495 +/- 6.416	-17.232 +/- 0.879	-148.997 +/- 12.346
βM	-194.741 +/- 26.780	-15.600 +/- 10.062	80.429 +/- 13.565	-18.648 +/- 1.566	-148.560 +/- 18.394
γM	-182.437 +/- 13.130	-6.963 +/- 8.272	74.621 +/- 10.076	-17.388 +/- 1.191	-132.167 +/- 11.079

CONCLUSION

This study provides a molecular insight into the interactions of α-mangostin (α-MG), β-mangostin (β-MG), and γ-mangostin (γ-MG) with TNF-α, a key inflammatory mediator in osteoarthritis (OA). Among the three derivatives, γ-MG demonstrated the highest binding affinity and the most favorable interaction profile with the TNF-α receptor, suggesting its potential as a superior inhibitor compared to α-MG and β-MG. The binding analysis revealed that γ-MG effectively mimics the interactions of the native ligand, engaging with key amino acids in the active site of the receptor, which could translate into a more potent suppression of TNF-α mediated inflammation. In contrast, α-MG and β-MG exhibited lower binding affinities, primarily due to suboptimal hydrogen bonding and weaker hydrophobic interactions. These results underscore the varying efficacy of mangostin derivatives in targeting TNF-α, highlighting γ-MG as the most promising candidate.

ACKNOWLEDGEMENTS

The authors would like to thank Poltekkes Kemenkes Makassar for the support of facilities so that the research can be carried out.

AUTHOR CONTRIBUTIONS

All the authors contributed significantly to this manuscript, participated in reviewing/editing and approved the final draft for publication. The research profile of the authors can be verified from their ORCID ids, given below:

A. Tang https://orcid.org/0000-0001-5415-4601
D.S.F. Ramadhan https://orcid.org/0000-0001-6257-7276
R. Dewi https://orcid.org/0000-0001-6382-8604
R. Muntu https://orcid.org/0000-0001-6730-4437
Nurisyah https://orcid.org/0000-0003-3934-2334

REFERENCES

1. S. Derry, P.J. Wiffen, E.A. Kalso, R.F. Bell, D. Aldington, T. Phillips, H. Gaskell, R. A. Moore, *Cochrane Database of Systematic Reviews*, **5(5)**, CD008609(2017), https://doi.org/10.1002/14651858.CD008609.pub2
2. N. Tatiya-Aphiradee, W. Chatuphonprasert, K. Jarukamjorn, *Biomedicine & Pharmacotherapy*, **111**, 705(2019), https://doi.org/10.1016/j.biopha.2018.12.142
3. P.A.S.S. Rodrigues, A.L. de Oliveira, K. Mattos Brandão, L.D.S.G. Landeiro, L.C. Calmon, J.V.A. Cruz, M.D.A. Silva, A.F.S. Rocha, D.S.C. Souza, A.T.A. de Moreira, J.O. Santos, T.M.B. dos Santos,

G.P. Pinheiro, Á.A.S. da Cruz Filho, C.A.V. de Figueiredo, P. de Moura Santos, R.D.S. Costa, *Gene*, **928**, 148804(2024), https://doi.org/10.1016/j.gene.2024.148804
4. Y. Gao, Y. You, P. Zhang, Y. Yu, Z. Xu, H. Wei, Z. Liu, R. Yu, G. Jin, H. Wang, S. Zhang, Y. Li, W. Li, *Communications Biology*, **7(1)**, 132(2024), https://doi.org/10.1038/s42003-024-05795-5
5. N.F. Zebua, N. Nerdy, A.W. Septama, D. Suryani, *Rasayan Journal of Chemistry*, **18(1),** 197(2025), http://doi.org/10.31788/RJC.2025.1819121
6. J. Remali, I. Sahidin, W.M. Aizat, *Frontiers in Plant Science*, **13**, 809497(2022), https://doi.org/10.3389/fpls.2022.809497
7. P. Tangpromphan, S. Palitsakun, A. Kaewchada, A. Jaree, *Case Studies in Chemical and Environmental Engineering*, **8,** 100537(2023), https://doi.org/10.1016/j.cscee.2023.100537
8. M. Askar, *Pharmacia*, **71(1)**, 1(2024), https://doi.org/10.3897/pharmacia.71.e129151
9. S.K. Burley, H.M. Berman, C. Bhikadiya, C. Bi, L. Chen, L. Di Costanzo, C. Christie, K. Dalenberg, J.M. Duarte, S. Dutta, Z. Feng, S. Ghosh, D.S. Goodsell, R.K. Green, V. Guranović, D. Guzenko, B.P. Hudson, T. Kalro, Y. Liang, R. Lowe, H. Namkoong, E. Peisach, I. Periskova, A. Prlić, C. Randle, A. Rose, P. Rose, R. Sala, M. Sekharan, C. Shao, L. Tan, Y.-P. Tao, Y. Valasatava, M. Voigt, J. Westbrook, J. Woo, H. Yang, J. Young, M. Zhuravleva, C. Zardecki, *Nucleic Acids Research*, **47(D1)**, D464(2019), https://doi.org/10.1093/nar/gky1004
10. N. Lolok, S.A. Sumiwi, D.S.F. Ramadhan, J. Levita, I. Sahidin, *Journal of Biomolecular Structure and Dynamics*, **42(4)**, 1952(2024), https://doi.org/10.1080/07391102.2023.2243519
11. D.S.F. Ramadhan, F. Siharis, S. Abdurrahman, M. Isrul, T.M. Fakih, *Journal of Biomolecular Structure and Dynamics*, **40(22),** 1(2021), https://doi.org/10.1080/07391102.2021.1959405
12. J. Ren, X. Yuan, J. Li, S. Lin, B. Yang, C. Chen, J. Zhao, W. Zheng, H. Liao, Z. Yang, Z. Qu, *Journal of the Chinese Chemical Society*, **67(1)**, 132(2020), https://doi.org/10.1002/jccs.201900148
13. A.W. Sousa da Silva, W.F. Vranken, *BMC Research Notes*, **5(1)**, 367(2012), https://doi.org/10.1186/1756-0500-5-367
14. J.V. Vermaas, D.J. Hardy, J.E. Stone, E. Tajkhorshid, A. Kohlmeyer, *Journal of Chemical Information and Modeling*, **56(6)**, 1112(2016), https://doi.org/10.1021/acs.jcim.6b00103
15. M.D. Smith, J.S. Rao, E. Segelken, L. Cruz, *Journal of Chemical Information and Modeling*, **55(12)**, 2587(2015), https://doi.org/10.1021/acs.jcim.5b00308
16. K. Baral, P. Adhikari, B. Jawad, R. Podgornik, W-Y. Ching, *Polymers*, **13(19)**, 3434(2021), https://doi.org/10.3390/polym13193434
17. A. Hicks, M. MacAinsh, H-X. Zhou, *Journal of Chemical Theory and Computation*, **17(9)**, 5920(2021), https://doi.org/10.1021/acs.jctc.1c00448
18. A. Golbraikh, M. Shen, Z. Xiao, Y-D. Xiao, K-H. Lee, A. Tropsha, *Journal of Computer-Aided Molecular Design*, **17(2–4)**, 241(2003), https://doi.org/10.1023/a:1025386326946
19. M.B. Kubitzki, B.L. De Groot, *Biophysical Journal*, **92(12)**, 4262(2007), https://doi.org/10.1529/biophysj.106.103101
20. R. Kumari, R. Kumar, OSDD Consortium, A. Lynn, *Journal of Chemical Information and Modeling*, **54(7)**, 1951(2014), https://doi.org/10.1021/ci500020m
21. R. Saini, S. Kumari, A. Bhatnagar, A. Singh, A. Mishra, *Scientific Reports*, **13(1)**, 8885(2023), https://doi.org/10.1038/s41598-023-33065-7
22. D. Hikmawati, T.M. Fakih, E. Sutedja, R.F. Dwiyana, N. Atik, D.S.F. Ramadhan, *Informatics in Medicine Unlocked*, **28**, 100844(2022), https://doi.org/10.1016/j.imu.2022.100844
23. J.M.J. Swanson, R.H. Henchman, J.A. McCammon, *Biophysical Journal*, **86(1)**, P67(2004), https://doi.org/10.1016/S0006-3495(04)74084-9
24. M.M. Damayanti, M. Rachmawati, E. Widiyastuti, Y. Kharisma, T.M. Fakih, A. Arfan, D.S.F. Ramadhan, *Rasayan Journal of Chemistry,* **Special Issue**, 158(2022). http://doi.org/10.31788/RJC.2022.1558192

[RJC-9104/2024]